Available online at www.sciencedirect.com
ScienceDirect
Applied Surface Science 254 (2008) 2771–2775
applied surface science
www.elsevier.com/locate/apsusc

Modeling the influence of the porosity of laser-ablated silicon films on their photoluminescence properties

M. Meunier *, J.-S. Bernier, J.-P. Sylvestre, A.V. Kabashin

Laser Processing Laboratory, Department of Engineering Physics, École Polytechnique de Montréal, C.P. 6079, Succ. Centre-ville, Montréal, Québec, Canada H3C 3A7

Received 30 June 2007; received in revised form 8 October 2007; accepted 10 October 2007
Available online 13 October 2007

Abstract

Nanostructured porous Si-based films produced by pulsed laser ablation (PLA) from a silicon target in residual helium gas can exhibit both size-dependent (1.6–3.2 eV) and fixed photoluminescent (PL) bands (1.6 and 2.2 eV) with their relative contributions depending on the film porosity. We study the influence of prolonged oxidation in ambient air on properties of the fixed PL bands, associated with oxidation phenomena, and their correlation with structural properties of the films. In addition, we propose a model describing the appearance of surface radiation states for oxidized films of various porosities. Our experiments and numerical simulations led to a conclusion that the 1.6 eV PL is due to a mechanism involving a recombination through the interfacial layer between Si core and an upper oxide of nanocrystals. This mechanism gives the optimal porosity of 73% for the most efficient production of 1.6 eV PL centers that is in excellent agreement with our experimental results.

PACS : 75.55.−m; 81.15.Fg

Keywords: Pulsed laser ablation; Nanostructured silicon; Visible photoluminescence; Porosity

1. Introduction

Nanostructured silicon (n-Si) is the focus of intensive research for more than 15 years due to its extremely promising properties for optoelectronics [1] and biosensing [2] applications. Nanostructured porous silicon [3] and Si-based films [3–7] are of great technological interest due to their capability to generate photoluminescence (PL) in the visible and UV range, which is not possible with Si in the bulk state. However, despite the efficient PL emission, mechanisms of PL are still in dispute. Here, several possibilities are still considered, including quantum confinement effects [3–8], SiO/Si interfacial layer [5,6], surface oxide defects [9], radiative recombinations in formed siloxene derivatives [10] and surface electronic states [11]. A clear identification of PL origin is complicated by the fact that different fabrication techniques, treatment procedures and investigation tools can lead to quite different properties of n-Si. In fact, each method brings novel nuances in structural or PL characteristics.

Laser ablation has shown itself as one of few efficient ''dry'' nanofabrication methods, whose advantage consists in excellent compatibility with silicon processing technology. The method consists in the ablation of a solid target by intense laser radiation, yielding to an ejection of its constituents and to the formation of nanoclusters, which are then deposited on a substrate to form a nanostructured film (for review, see [12]). Although laser-ablated films were found to exhibit strong PL in UV–vis range [13–24], results of different groups were rather contradictory. Makimura et al. [16,17], Yoshida and co-workers [15,18] reported the presence of nearly fixed PL peaks at 1.5–1.7, 2.1–2.3 and 2.7 eV from films, produced by the ablation of Si in He and their subsequent annealing. Size-independence and a strong relation to oxidation phenomena lead them to attribute these signals to surface oxide defects [9] or SiO/Si interfacial layer [5,6]. In contrast, Patrone et al. [19,20] reported size-dependent PL spectra from films, produced by the ablation of Si in helium, which was in good agreement with the quantum confinement mechanism [3]. Later, we showed that such a discrepancy of results could be due to different film porosities in these studies [24]. Low-porous films, deposited at reduced pressures of helium ($P < 1.5$ Torr), exhibited size-dependent PL with peak positions

* Corresponding author. Tel.: +1 514 340 4711x4971.
E-mail address: Michel.meunier@polymtl.ca (M. Meunier).

0169-4332/$ – see front matter
doi:10.1016/j.apsusc.2007.10.016

between 1.6 and 2.15 eV, similar to Ref. [19,20], while films of higher porosity, deposited at $P > 1.5$ Torr, provided only spectra with fixed peaks around 1.6 and 2.2–2.3 eV, similar to ones observed in Ref. [15–18]. We then proposed that porosity was one of the key factor controlling the contribution of different mechanisms [24]. Dense and self-coagulated structures of low-porous films prevented the oxidation contributing to a relative predominance of core crystal-based mechanisms such as the quantum confinement [3], while highly porous structures enhanced the surface area, which was subjected to oxygen, favoring oxidation-related mechanisms [5,6,9]. However, many aspects related to the impact of oxidation phenomena remained unclear. In particular, none of the previous studies of nanostructured film properties considered the effect of porosity on the formation of PL centers.

In this paper, we reexamine PL signals associated with oxidation-based mechanisms and study their correlation with the porosity of the synthesized nanostructured films. In addition, we develop a model, explaining the formation of PL centers due to a prolonged film oxidation.

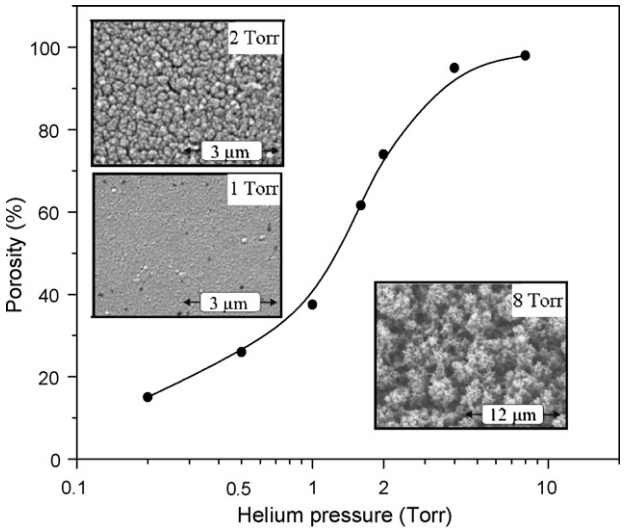

Fig. 1. Porosity of the films estimated from SXRR curves as a function of helium pressure during the deposition. Insets show typical SEM images of the films deposited under different pressures.

2. Experimental

For the fabrication of Si-based films, we used a methodology described in detail in Refs. [22–24]. Briefly, radiation of a pulsed KrF laser ($\lambda = 248$ nm, pulse length = 15 ns FWHM, repetition rate = 30 Hz) was used for the ablation of material from a rotating Si target ((1 0 0), N-type, resistance 10 Ω cm). The radiation was focused on a focal spot 2 mm × 1 mm on the target at the incident angle of 45° giving the radiation intensity of about 5×10^8 W/cm^2. The substrates, identical to the target, were placed on a rotating substrate holder at 2 cm from the target. The experimental chamber was pumped down to $P = 2 \times 10^{-7}$ Torr before filling with helium (purity 99.99995%) for a deposition at a constant pressure P ranging between 0.05 and 10 Torr. The film thickness after several thousands laser shots was 100–700 nm.

PL spectra were recorded on a double spectrometer (U100, Instruments SA) using 488 nm radiation of an Ar^+ laser with power density of 30 W/cm^2 as a source and a GaAs photomultiplier as the detector. Scanning electron microscopy (SEM), X-ray diffraction (XRD) and specular X-ray reflectivity (SXRR) spectroscopies were used to examine structural properties of the films [24]. In addition, X-ray photoemission spectroscopy (XPS) was used to determine the surface layer composition.

3. Silicon films porosity and photoluminescence properties

Our experiments showed that the porosity of the laser-ablated films increased gradually as the pressure of helium was increased during the pulsed laser ablation experiment. Typical SEM images of the films deposited under different pressures of He are shown in insets of Fig. 1. Here, one can see that the deposition under 1 Torr resulted only in some germs of roughness, while the experiment under 2 Torr provided a developed porous structure with pore size of about 50–100 nm. Further pressure increase up to 4 Torr led to a formation of web-like aggregations of particles. Note that under $P < 1$ Torr the roughness details were too small to be detected by our SEM system. The porosity of the films was measured by specular X-ray reflectivity [25] using a simple powder X-ray diffractometer (the precision of the porosity measurement using this method is about 10%). The methodology and details of porosity measurements can be found in Ref. [24]. Fig. 1 summarizes the porosity measurements for laser-ablated films deposited under different pressures P. Here, a tendency of the porosity enhancement with the pressure increase is quite clear for $P < 2$ Torr, while for higher pressures the porosity always exceeds 95%. The increase of the film porosity could be explained by a change of conditions of nanocluster formation under an increase of the helium pressure. It is known that originally the material is ablated in the form of atoms and smallest nanoscale clusters [12]. Collisions with light helium atoms cause a cooling of the clusters and their size enlargement. Under relatively low pressures, a number of collisions are probably not sufficient to condense and crystallize the clusters in gaseous phase. Therefore, the clusters in the gas phase are relatively hot and crystallize when they arrive on the substrate forming a dense and well-packed crystalline film. In contrast, under high pressures, more frequent collisions lead to a fast cooling and more effective condensation of clusters in the gaseous phase. As a result, they arrive on the substrate with larger size, being partially crystallized and having an arbitrary shape, which causes a formation of highly porous layers and even web-like agglomerations. It should be noted that the above-stated assumption is confirmed by results of a recent study [26], in which a clear correlation between the increase of the film porosity and the decrease of energy of ejected species was observed. Such a decrease of the energy was related to more frequent collisions with ambient gas under the increase of the background pressure.

Our experiments showed that PL properties were quite different for films of different porosities. As shown in Fig. 2a, the low-porous (<50%) films exhibited various PL bands between 1.6 and 2.2 eV with the PL peak position depending on the film porosity. As we showed in Ref. [23], the blue-shift of the PL position was also accompanied by a decrease of the mean size of nanoscale grains forming the film skeleton, suggesting the quantum confinement [3] as the main mechanism of PL. These results suggest that although the porosity might improve the passivation of dangling bonds for films of higher porosity, it could not bring new mechanisms for these relatively dense and well-coagulated films. In contrast, highly porous (>60%) films exhibited peaks in the red and green range, whose position did not depend on the nanocrystal size. The red band (1.6–1.8 eV) appeared just after the exposition of the films to ambient air, while the green one (2.1–2.2 eV) appeared after a prolonged oxidation of films in humid air. Originally, signals of the first band were weak and situated near 1.7–1.8 eV. Then, a prolonged oxidation of the films led to a red-shift of the peak toward 1.6 eV and the one–two orders increase of its amplitude, as shown in Fig. 3. Similar effect took place under the removal of the upper oxide layer by 5% HF solution. After this treatment, the red band again exhibited a weak peak at 1.7–1.8 eV, which was then reinforced and shifted toward 1.6–1.65 eV, similar to spectra shown in Fig. 3. These properties were in good agreement with previous studies of Si-based films, deposited in an oxygen-free atmosphere [5,6,27]. The origin of the green PL was studied by many authors and generally attributed to defects in the SiO_2 structure [9]. In contrast, the origin of 1.65–1.8 eV PL is not yet completely understood. Kanemitsu et al. [5,6] proposed a model, in which the generation of this band was related to an exciton confined in an interfacial layer SiO_x between the Si core and the upper SiO_2 oxide shell. However, conditions of formation of radiation states, responsible for such PL, are still not clear.

Summarizing the obtained experimental data, the integral intensity of PL signal as a function of film porosity after many weeks of oxidation in ambient air shows a clear maximum at 73% porosity. The fact that the optimal porosity is relatively high is not trivial, taking into account surface-proportional character of contribution of these mechanisms, while the maximal surface-to-volume ratio is known to take place for lower porosities of 50%. In order to understand the physics of formation of PL centers and link them to the film porosity, we developed a model, taking account of oxidation effects. This model is presented in the next section.

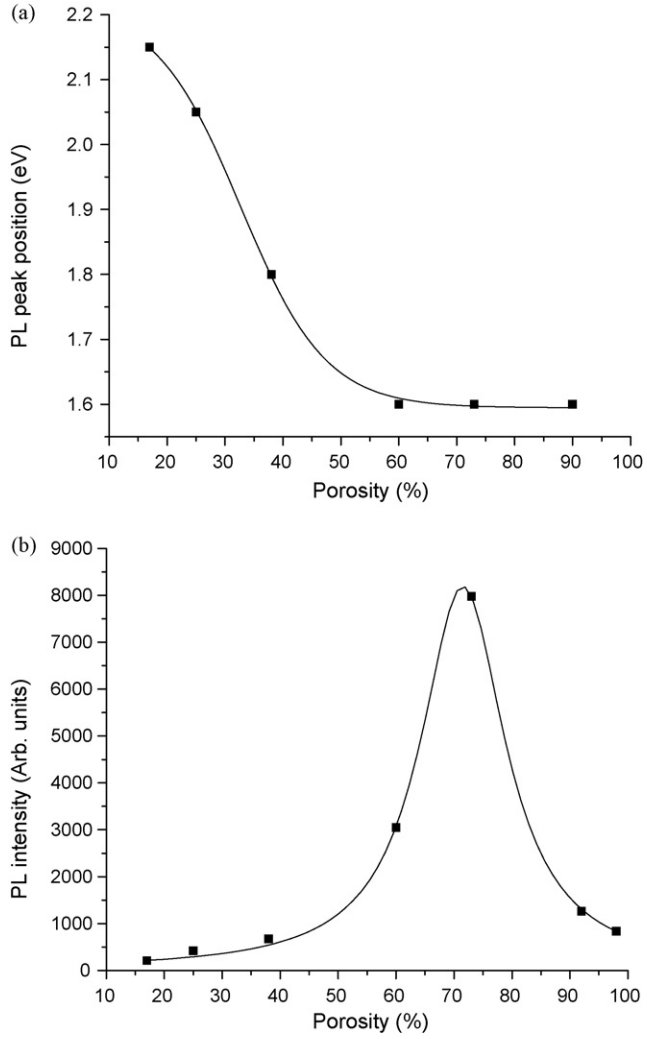

Fig. 2. (a) PL peak position as a function of the porosity of laser-ablated films; (b) integral intensity of PL signal as a function of film porosity after 6 weeks of oxidation in ambient air.

4. Modeling the effect of porosity

In our model, we assume that every evaporated nanoparticle is deposited as an elementary block of the same size. We consider these blocks to be 5 nm × 5 nm × 5 nm in size, which is in good agreement with the average dimension of nanoclusters produced by laser ablation [15–24]. Then, the blocks are deposited into an 3-dimensional matrix of fixed size L_x, L_y and L_z, where the z-axis represents the film thickness and the x- and y-axis, both perpendicular to the z coordinate,

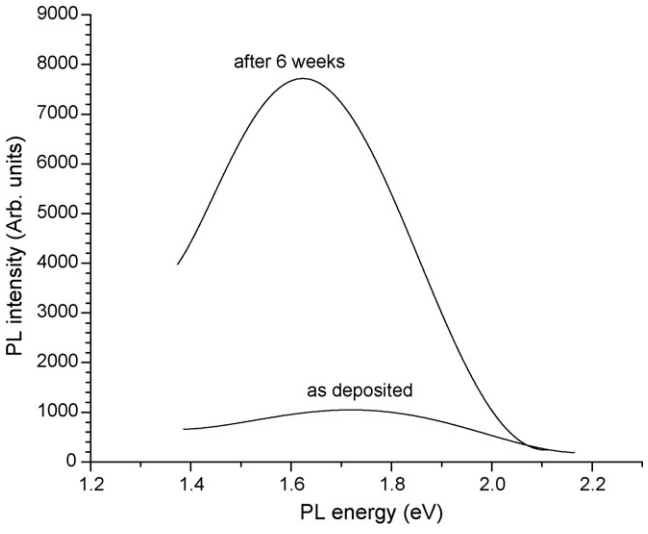

Fig. 3. Typical PL spectra of highly porous (73%) films just after the fabrication and after 6 weeks of natural oxidation in ambient air.

represent the film width. To study large area thin films, we use periodic boundary conditions in the x–y plane. We assume that all blocks are deposited casually similarly to the Tetris random probability algorithm. To simulate the film generation, we set two rules to determine at which position a given block will be deposited:

(1) If the position z–1 is occupied, the block will rest at the z position;
(2) If a neighboring position in the plane x–y is already occupied by another block, the block being deposited has a non-zero probability to stick to the side of its neighbor even though the position directly below is unoccupied. This probability that we can assimilate to a sticking factor has a direct influence on the final porosity of the film. Obviously, as the stick-probability gets closer to one, the porosity increases.

The deposition part of the simulation terminates when it is impossible to add a supplementary block inside the volume defined by the 3-dimensional matrix. Normally, this condition occurs when the z upper layer at L_z is completely filled by blocks. Consequently, to represent the physical film, not constrained in thickness, we remove the top layer once the deposition terminates. For a sticking probability of 0 (porosity of 0), the 3-dimensional matrix is completely filled by $N_0 = L_x L_y L_z$ blocks. For non-zero sticking probability, the solid is formed by N_{blocks} and the porosity can be obtained as follows:

$$\text{Porosity} = 100\% \times \frac{(N_0 - N_{\text{blocks}})}{N_0}$$

The model relies on the fact that the oxygen in the air can diffuse into the porous structure and oxidize internal surfaces, thus creating PL defect centers. Of course, if some pores are imbedded into the solid, the oxygen would not reach these internal surfaces which should be ignored in the calculation. Therefore, we need to estimate the total internal surface that is only exposed to air. To do so, we identify every hollow region within the matrix with its point of contact at the film surface, and thus determine all ''effective channels''. To consider this effect, we create a comparative structure in which all elementary spatial units are initially occupied by blocks. We then scan the upper layer of the first structure to identify all empty locations responsible for the oxygen access to inner layers, and remove corresponding blocks from the second structure. After analyzing all layers we can identify all empty pores which do not have access to air and exclude them from our calculation. We can then calculate the number N of nanocrystal facets exposed to air. Then, knowing the relative percentage of the effective channels, we can calculate the efficiency of formation of PL centers by oxidation-related mechanisms. The intensity of PL emission obeys Beer–Lambert formula:

$$I_e = I_i(1 - P_r)\, f(N) \exp(-\alpha_e n d) \tag{2}$$

where I_e is the emitted intensity, I_i the incident intensity. P_r the reflection coefficient, α_e the absorption coefficient, n the number of crossed layers, and d the dimension of a block. Finally, $f(N)$ is a function related to the oxidized surface of the emitters.

For the mechanism proposed by Kanemitsu, PL centers are formed through the oxidation of nanocrystals of ''effective channels''. The oxidation leads to a simultaneous creation of radiation states on both sides of the interfacial layer between the Si-core and the SiO_2 oxide shell (virtual sheet). The PL emission at energy $E_{\text{upper}} - E_{\text{ground}}$ is due to a transition between an upper and ground states. However, it is not clear whether the formation of such centers giving rise to these two states is mutually dependent. We reason that in the case of simultaneous formation of the centers, the function $f(N)$ must be proportional to a number of nanocrystal facets subjected to the oxidation N, while in the case of independent center formation it must be proportional to N^2. We performed calculations in the proposed model for both situations and the results are presented in Fig. 4(a) and (b), respectively. Here, one can see that the first ''dependent case'' provides optimal conditions for the formation of PL centers at porosities 61%, which does not agree with our experimental data. In contrast, the second case provides such an optimum at 73%, which is in

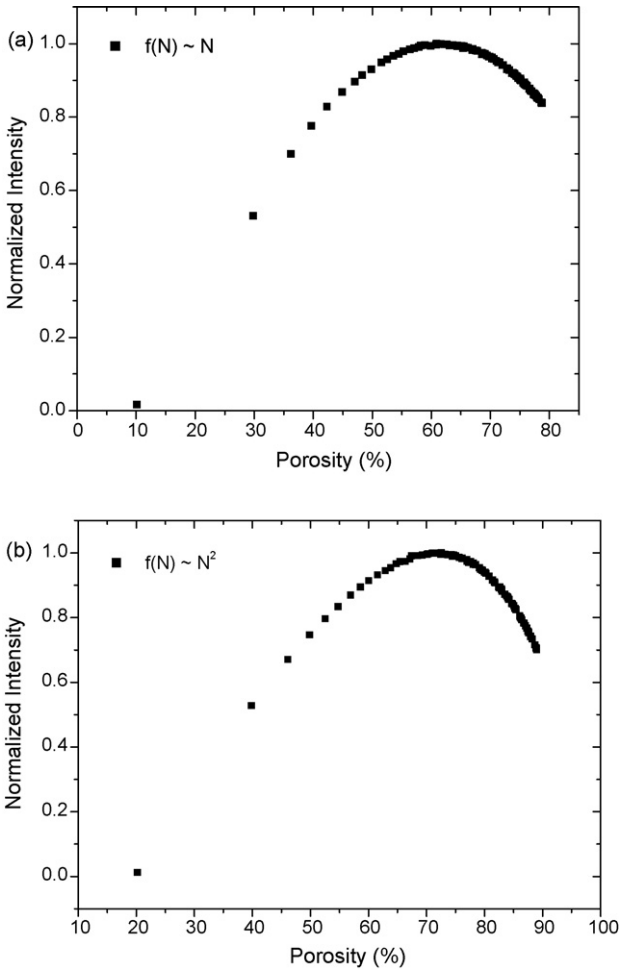

Fig. 4. Simulated PL integrated intensity as a function of the porosity for nanocluster Si films. In (a) and (b) we show cases of mutually dependent and independent formations of radiation states, respectively.

excellent agreement with results presented in Fig. 2. Thus, our modeling suggests that this porosity of 73% provides optimal conditions for oxygen-related mechanisms, if we assume that ground and upper radiation states are formed independently.

5. Conclusions

Si/SiO_x nanostructured films fabricated by a pulsed laser ablation in helium residual gas exhibit visible PL that drastically changes upon oxidation phenomena. These phenomena become dominant in the formation of PL centers giving rise to a maximum PL emission when the film porosity is 73%. Simulation results based on our model suggest that this porosity optimal condition corresponds to an independent formation of radiation states due to air oxidation phenomena. We hope that this important data will help to develop a self-consistent model of PL center formation by oxidation phenomena.

Acknowledgements

The authors are grateful to Prof. Richard Leonelli for assistance during PL measurements and to Dr. D.-Q. Yang for useful discussions. This work was supported by the NSERC (Natural Science and Engineering Research Council) of Canada and Canada Research Chair on Laser micro/nano-engineering of materials.

References

[1] L. Pavesi, L. Dal Negro, C. Mazzolenl, G. Franzo, F. Priolo, Optical gain in silicon nanocrystals, Nature 408 (2000) 440–444.
[2] V.S.-Y. Lin, K. Motesharei, K.P.S. Dancil, M.J. Sailor, M.R. Ghadiri, Science 278 (1997) 840.
[3] L.T. Canham, Appl. Phys. Lett. 57 (1990) 1046.
[4] H. Takagi, et al. Appl. Phys. Lett. 56 (1990) 2379.
[5] Y. Kanemitsu, Phys. Rev. B 48 (1993) 12357.
[6] Y. Kanemitsu, T. Ogawa, K. Shiraishi, K. Takeda, Phys. Rev. B 48 (1993) 4883.
[7] E. Edelberg, S. Bergh, R. Naone, M. Hall, B.S. Aydil, Appl. Phys. Lett. 68 (1996) 1415.
[8] K.S. Min, K.V. Shcheglov, C.M. Yang, H.A. Atwater, M.L. Brongersma, A. Polman, Appl. Phys. Lett. 69 (1996) 2033.
[9] S.M. Prokes, Appl. Phys. Lett. 62 (1993) 3244.
[10] M.S. Brandt, H.D. Fuchs, M. Stutzmann, J. Weber, M. Cardona, Solid State Commun. 81 (1992) 307–312.
[11] M.V. Wolkin, J. Jorne, P.M. Fauchet, G. Allan, C. Delerue, Phys. Rev. Lett. 82 (1999) 197–200.
[12] A.V. Kabashin, M. Meunier, Laser ablation-based synthesis of nanomaterials, in: J. Perrière, E. Millon, E. Fogarassy (Eds.), Recent Advances in Laser Processing of Materials, Elsevier, 2006, pp. 1–36.
[13] E. Werwa, A.A. Seraphin, L.A. Chiu, C. Zhou, K.D. Kolenbrander, Appl. Phys. Lett. 64 (1994) 1821.
[14] I.A. Movtchan, R.W. Dreyfus, W. Marine, M. Sentis, M. Autric, G. Le Lay, N. Merk, Thin Solid Films 255 (1995) 286.
[15] Y. Yamada, T. Orii, I. Umezu, Sh. Takeyama, T. Yoshida, Jpn. J. Appl. Phys., Part 1 35 (1996) 1361.
[16] T. Makimura, Y. Kunii, K. Murakami, Jpn. J. Appl. Phys., Part 1 35 (1996) 4780.
[17] T. Makimura, Y. Kunii, N. Ono, K. Murakami, Appl. Surf. Sci. 127–129 (1998) 388.
[18] I. Umezu, K. Shibata, S. Yamaguchi, A. Sugimura, Y. Yamada, T. Yoshida, J. Appl. Phys. 84 (1998) 6448.
[19] L. Patrone, D. Nelson, V.I. Safarov, M. Sentis, W. Marine, S. Giorgio, J. Appl. Phys. 87 (2000) 3829.
[20] W. Marine, L. Patrone, B. Luk'yanchuk, M. Sentis, Appl. Surf. Sci. 154–155 (2000) 345.
[21] N. Suzuki, T. Makino, Y. Yamada, T. Yoshida, S. Onari, Appl. Phys. Lett. 76 (2000) 1389.
[22] A.V. Kabashin, M. Charbonneau-Lefort, M. Meunier, R. Leonelli, Appl. Surf. Sci. 168 (2000) 328.
[23] A.V. Kabashin, M. Meunier, R. Leonelli, J. Vac. Sci. Technol. B 19 (2001) 2217.
[24] A.V. Kabashin, J.-P. Sylvestre, S. Patskovsky, M. Meunier, J. Appl. Phys. 91 (2002) 3248–3254.
[25] L.T. Parratt, Phys. Rev. 95 (1954) 359.
[26] D. Riabinina, M. Chaker, F. Rosei, Appl. Phys. Lett. 89 (2006) 131501.
[27] S. Botti, R. Coppola, F. Gourbilleau, R. Rizk, J. Appl. Phys. 88 (2000) 3396.